Physica Medica 60 (2019) 120–126

Contents lists available at ScienceDirect

Physica Medica

journal homepage: www.elsevier.com/locate/ejmp

# An in silico planning study comparing doses and estimated risk of toxicity in 3D-CRT, IMRT and proton beam therapy of patients with thymic tumours

Anders Lidestål[a,*], Gracinda Mondlane[a,b], Michael Gubanski[a], Pehr A. Lind[b,c], Albert Siegbahn[b,c]

[a] Department of Oncology-Pathology, Karolinska Institutet, Stockholm, Sweden
[b] Department of Oncology, Södersjukhuset, Stockholm, Sweden
[c] Department of Clinical Science and Education, Karolinska Institutet, Södersjukhuset, Stockholm, Sweden

ARTICLE INFO

*Keywords:*
Thymic tumour
Scanned-proton beams
Dosimetric comparison
Normal tissue complication probability,
intensity-modulated radiation therapy

ABSTRACT

*Purpose:* To compare the dose distributions produced in patients (pts) treated for thymic tumours with spot-scanning proton beam therapy (PBT) implemented with single-field uniform dose (SFUD), intensity-modulated radiation therapy (IMRT) and three-dimensional conformal photon-beam based radiotherapy (3D-CRT).
*Methods:* Twelve pts, treated with 3D-CRT, were included. Alternative IMRT and SFUD plans were constructed. The IMRT plans were created using a setup with beams incident from 5 to 6 different angles. For the SFUD plans, a field-specific planning target volume (PTV) was created for each patient and a clinical target volume (CTV)-based robust optimization was performed. A robustness evaluation was performed for the CTV for all SFUD plans. A dosimetric evaluation was conducted for the doses to the CTV and organs at risk (OARs) for all plans. The normal tissue complication probability (NTCP), for different endpoints, was calculated using the Lyman-Kutcher-Burman (LKB)-model and compared between plans.
*Results:* SFUD was associated with significantly lower mean doses to the oesophagus, the heart, the left anterior descending coronary artery (LAD), lungs and breasts compared to 3D-CRT and IMRT. The maximum dose given to the spinal cord was significantly lower with SFUD. The risks for pneumonitis, esophagitis and myelopathy were significantly reduced in the SFUD plans.
*Conclusions:* The present study showed dosimetric advantages of using scanned-beam PBT for the treatment of thymic tumours, as compared to 3D-CRT and IMRT, especially in regard to lower doses to the oesophagus and lungs. The risk of toxicity was reduced with SFUD.

## 1. Introduction

Thymic tumours, *i.e.* thymoma and thymic carcinoma, derive from the epithelial cells of the thymus gland. Thymic tumours may be non-invasive (WHO Type A thymoma) or show loco regional invasive, or even metastatic traits (WHO Type B thymomas and Type C thymic carcinomas, respectively) [1]. Thymectomy is the main, and sometimes definitive, treatment. Patients (pts) with positive surgical margins, gross residual disease, tumour recurrence or unresectable tumours, may be treated with radiotherapy (RT), in a neo-/adjuvant, salvage or definitive setting. Prescribed doses depend on the clinical indication, with lower doses given to pts with minimal or positive surgical margins (45–60 Gy) and higher doses to patients with gross residual disease or unresectable tumours (60–70 Gy) [2]. Radiotherapy is often combined with platinum-based chemotherapy [2].

Due to its location in the anterior mediastinum, the thymus is closely adjacent to several critical organs, such as heart, lungs, oesophagus and spinal cord. Several studies on RT in thoracic tumours, *e.g.* breast cancer, lymphoma, lung-, and oesophageal cancer, have shown a wide range of acute and long-term toxicities, *e.g.*, pneumonitis, pericarditis, esophagitis, myelitis and cardiovascular events [3–6]. As the long-term survival for many thymoma pts is excellent, avoidance of severe RT-related side effects is vital.

A small number of studies have shown dosimetric advantages when using proton beam therapy (PBT) in the treatment of thymic tumours as compared to photon RT, especially with regard to doses to the organs at risk (OAR) [7,8]. In the present study, we evaluate the dosimetric- and NTCP-outcomes for 12 patients treated for thymoma, or thymic carcinoma, comparing spot-scanning PBT implemented with the single-field uniform dose (SFUD) technique and photon beam RT performed with three-dimensional conformal radiotherapy (3D-CRT) and intensity-modulated radiation therapy (IMRT). Multi-field optimization was not

* Corresponding author at: Karolinska Institutet, Department of Oncology-Pathology, Karolinska University Hospital, Z1:00, 171 76 Stockholm, Sweden.
*E-mail address:* anders.lidestahl@sll.se (A. Lidestål).

https://doi.org/10.1016/j.ejmp.2019.03.028
Received 14 August 2018; Received in revised form 26 March 2019; Accepted 27 March 2019
Available online 30 March 2019
1120-1797/ © 2019 Published by Elsevier Ltd on behalf of Associazione Italiana di Fisica Medica.

**Table 1**
Patient characteristics.

| Pt | Sex (M/F) | Age (years) | Surgery (y/n) | Margin | Chemotherapy | Histology (WHO) |
|---|---|---|---|---|---|---|
| 1 | M | 76 | n | – | carboplatin/etoposide | * |
| 2 | F | 65 | y | R1 | none | B3 |
| 3 | M | 64 | y | R0 | none | C |
| 4 | M | 63 | y | R1 | none | B3 |
| 5 | F | 59 | y | R1 | none | B2/3 |
| 6 | M | 56 | n | – | cisplatin/docetaxel | C |
| 7 | M | 53 | y | R0 | none | B3 |
| 8 | M | 52 | y | R1 | cisplatin/etoposide | B2/3 |
| 9 | M | 49 | y | R1 | cisplatin/etoposide | B3 |
| 10 | M | 73 | n | – | carboplatin/etoposide | B3 |
| 11 | M | 82 | y | R1 | none | B2/3 |
| 12 | M | 74 | y | R0 | carboplatin/etoposide | C** |

* biopsy showed infiltrative thymoma, tumour was not classified according to WHO.

** biopsy showed thymic cancer, pt received neoadjuvant chemotherapy and RT, surgical specimen after thymectomy showed no sign of vital tumour.

used due to uncertainties in the produced dose distributions, caused by possible organ movement, associated with this method.

## 2. Material and methods

The Regional Medical Ethics Committee has approved this study.

### 2.1. Patient, tumour and treatment characteristics

Twelve pts with thymic tumours (eight pts with WHO Type B2-3 thymomas, three pts with WHO Type C thymic carcinomas, and one pt with an infiltrative thymic tumour, which was not classified according to WHO, in the pathology report), who received 3D-CRT at our Institution, were included (Table 1). Ten pts were male, and the median age was 63.5 years (range: 49–82 years). Thymectomy was performed in 9 pts, whereas 3 pts were assessed as inoperable, and their histological diagnosis was based on biopsy. Six pts were treated with chemotherapy. RT was performed in a post-operative setting in 8 pts, as neo adjuvant treatment before surgery in 1pt, and as definitive treatment in 3 pts.

### 2.2. Set up and structure delineation

All patients underwent a pre-treatment planning CT-scan in a standardized supine position. An oncologist performed structure delineation on the CT image sets. There was not any gross tumour volume (GTV) remaining in the post-operative patients. The clinical target volume (CTV) covered the visible mass on the pre-operative CT image sets, and included possible residual disease on the post-surgery CT image sets. An isotropic expansion margin of 0.7 cm was added to the CTV to create the planning target volume (PTV) used for photon treatments (the PTV margin was based on recorded values for positioning uncertainty in this area for fixation on wing board without the use of a vacuum cushion, at our institution). The volumes of the CTV and the PTV for the pts included in this study are shown in Table 2. The delineation of OARs included both lungs excluding the CTV, heart, spinal cord, oesophagus, left anterior descending coronary artery (LAD), skin and both breasts (in both male and female pts). The spinal cord encompassed all the extension along the axially irradiated area.

### 2.3. Treatment planning

The treatment planning for photon- and proton-beam therapy was performed on the Eclipse™ treatment planning system (TPS) version 13.7 (Varian Medical Systems, Palo Alto, California). The 3D-CRT photon plans were prepared with 3 to 5 incident photon beams, (energies of 6, 15 and 18 MV) delivered by a Varian linear accelerator. The treatment was delivered 5 days a week in daily fractions between 1.8 Gy (RBE) (1pt) and 2 Gy (RBE) (11pts), and the total prescribed dose ranged between 50 and 60 Gy (RBE) (Table 2). The plan objective was to deliver doses between 95% and 107% of the prescribed dose to the PTV. The dose-volume constraints used for the OARs were as follow: the maximum allowed dose given to the spinal cord was set to 48 Gy (RBE), V20 for the lung(-)CTV should be below 35% of the total lung volume and the mean dose given to the whole oesophagus should not exceed 45 Gy (RBE). For the heart and the LAD, attempts were made to keep the dose as low as possible. The dose calculation was made using the analytical anisotropic algorithm (AAA). The clinical 3D-CRT plans used for the actual patient treatment were used as reference in the plan comparison. In addition, photon-based IMRT plans were retrospectively created for comparisons with the SFUD plans. These plans were also prepared in Eclipse™ TPS, using 6 MV photon beams produced by a Varian linear accelerator. Similar plan objectives and OAR constraints as for the 3D-CRT plans were also used to create the IMRT plans.

**Table 2**
Volumes of the CTV and PTV, the fraction doses and the number of fractions used for planning with 3D-CRT, IMRT, and SFUD for all patients.

| Patient # | Fx*. Dose (Gy (RBE)) | Number of fxs | CTV ($cm^3$) | PTV ($cm^3$) |
|---|---|---|---|---|
| 1 | 2 | 30 | 554 | 834 |
| 2 | 2 | 28 | 290 | 574 |
| 3 | 2 | 28 | 318 | 756 |
| 4 | 2 | 28 | 170 | 400 |
| 5 | 2 | 28 | 257 | 525 |
| 6 | 2 | 30 | 305 | 596 |
| 7 | 2 | 27 | 132 | 451 |
| 8 | 2 | 28 | 115 | 311 |
| 9 | 2 | 28 | 153 | 369 |
| 10 | 1.8 | 30 | 80 | 498 |
| 11 | 2 | 30 | 130 | 351 |
| 12 | 2 | 25 | 760 | 1246 |

* fx = fraction.

The planning for PBT was done using spot-scanning beams with kinetic energies between 60 and 230 MeV generated in an IBA machine (Ion Beam Applications, S.A., Louvain-La-Neuve, Belgium). The plans were prepared using the SFUD method. To ensure dose coverage of the part of the PTV, which was located closer to the patient surface, a range shifter of water equivalent thickness of 3.5 $g/cm^2$ was used. The treatment planning constraints used for 3D-CRT planning were also adopted for the SFUD planning. A two-beam configuration was used for proton irradiation. The field-specific PTV (fsPTV) tool available in the Eclipse™ TPS was used to design field-specific PTVs, which were then used for spot positioning. To reduce dose perturbations caused by sternal metal clips, the clips were delineated and assigned the same Hounsfield units as for the adjacent bone [9]. A CTV-based robust optimisation was thereafter performed accounting for an isotropic setup uncertainty of 0.7 cm and a proton range uncertainty of 3.5%. This resulted in one nominal plan (without perturbations) and 12 simulated plans with perturbed dose distributions. The dose calculation was done using the proton convolution superposition algorithm (PSC) and the optimisation was conducted with the Nonlinear Universal Proton Optimizer (NUPO) algorithm, both available in Eclipse™ TPS. To account for the relative biological effectiveness (RBE) of proton beams, a generic RBE of 1.1 was assumed [10].

### 2.4. Plan evaluation

A robustness evaluation of the SFUD plans was performed based on the robustness criteria set for the CTV: D90 ≥ 95% for all the simulated scenarios and D95 ≥ 95% for at least 10 of the 12 simulated robustness scenarios; for the spinal cord the V48 Gy (RBE) = 0% for all the

scenarios. For the 3D-CRT, IMRT and the SFUD plans, the D98 and the D2 of the CTV were registered. The homogeneity Index [11] was also calculated for the CTV for all patients and plans. For the OARs, the dose-volume values obtained in the 3D-CRT and IMRT plans were compared with the values obtained in the nominal SFUD plans and with the dosimetric values obtained in the worst-case scenario for the OARs in the SFUD plans (the scenario representing the highest dose-volume curve).

### 2.5. Assessment of NTCP

The assessment of NTCP was done using the Lyman-Kutcher-Burman (LKB) model shown in Equation (1) [12,13].

$$NTCP = \frac{1}{\sqrt{2\pi}} \int_{-\infty}^{t} \exp\left(-\frac{x^2}{2}\right) dx \quad (1)$$

Where,

$$t = \frac{D - TD_{50}(1) \bullet v^{-n}}{m \bullet TD_{50}(1) \bullet v^{-n}} \quad (2)$$

$TD_{50}(1)$ is the tolerance dose which leads to 50% complication probability after uniform whole organ irradiation; $v$ is the fractional volume irradiated with a uniform dose $D$, in this study chosen to be the maximum dose ($D_{max}$) received by the individual OAR; $n$ and $m$ are model parameters which describe the volume dependence of the NTCP and the slope of the dose response curve, respectively. To take the non-homogeneous dose distribution in the OARs into account, the effective-volume method [12] was used. With this method, the DVH obtained for an OAR was converted to the equivalent DVH, which would be obtained after uniform irradiation of an effective volume$v$ of the OAR with a dose equal to $D_{max}$. The LKB-model parameters used and the biological endpoints considered in the NTCP calculations are shown in Table 3. The values of the LQ-model parameter $\alpha/\beta$ used for the different OARs are also presented.

### 2.6. Statistics

A two-sided Wilcoxon signed-rank test was used to compare dosimetric outcomes and the estimated NTCPs between the SFUD plans and the two photon-based plans (3D-CRT and IMRT) for each patient. A $p$-value $< 0.05$ was considered statistically significant.

## 3. Results

### 3.1. Dosimetric comparison

For all pts, the robustness criteria set for the CTV and spinal cord were met with the SFUD plans. The planning objective for the PTV (3D-CRT plans) and the constraints for the OARs (3D-CRT and SFUD plans) were also respected. Typical dose distributions obtained with 3D-CRT and SFUD plans are shown in Fig. 1, for a representative patient case. The obtained DVHs for the CTV and the OARs with the 3D-CRT and the SFUD plans are also presented for this patient (Fig. 2).

For the 3D-CRT, IMRT and the SFUD plans, no significant difference

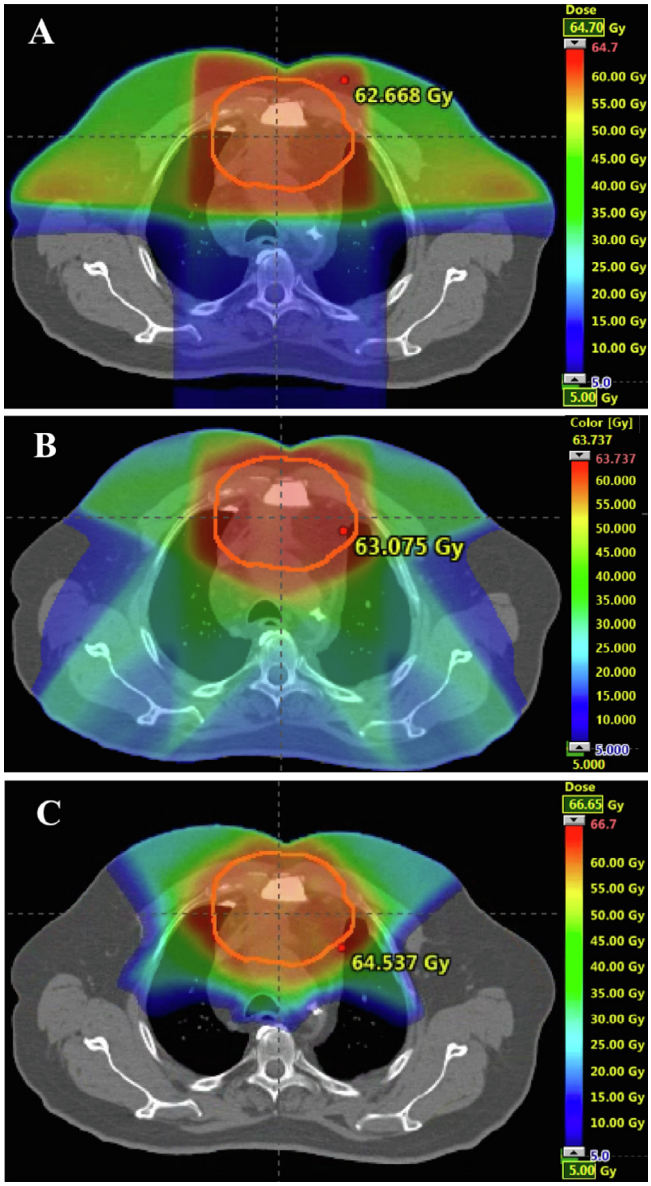


**Fig. 1.** Dose distributions in the axial plane for the 3D-CRT (A), IMRT (B) and SFUD (C) plans in a representative patient (patient #1).

was observed between the obtained values of the HI: 0.08 (IQR: 0.07 – 0.08), 0.06 (IQR: 0.06 – 0.08) and 0.07 (IQR: 0.06 – 0.08), respectively ($p > 0.05$). For the OARs, the nominal SFUD plans were associated with significantly lower values of the dose-volume metrics for the spinal cord ($D_{max}$), oesophagus ($D_{mean}$ and V30), heart ($D_{mean}$, V5, V30 and V45), LAD ($D_{mean}$), lung excluding the CTV ($D_{mean}$, V5 and V20) and for the total breast ($D_{mean}$), compared to both the 3D-CRT and IMRT ($p < 0.05$), see Table 4. There was no significant difference between the maximum dose given to the oesophagus, LAD, skin and total breast

**Table 3**
Values of the LKB-model parameters ($n$, $m$ and $TD_{50}$), the corresponding endpoints and the LQ-model parameter $\alpha/\beta$ for the different OARs studied.

| *Organ* | *n* | *m* | *$TD_{50}$ (Gy)* | *Endpoint* | *$\alpha/\beta$(Gy)* | *Sources* |
|---|---|---|---|---|---|---|
| Heart | 0.636 | 0.13 | 50.6 | Pericarditis | 3 | Martel et al. [40]. |
| Oesophagus | 0.44 | 0.32 | 51.0 | Grade 2 or greater acute esophagitis | 3 | Chapet et al. [41]. |
| Skin | 0.38 | 0.14 | 39.0 | Radiation-induced skin toxicity (RIST) | 3 | Pastore et al. [42]. |
| Lung | 1 | 0.41 | 29.9 | Symptomatic R. Pneumonitis | 3 | Semenenko & Li [43]. |
| Spinal cord | 0.05 | 0.175 | 66.5 | Radiation myelitis | 0.87* | Burman et al. [44]. |

* Value of the $\alpha/\beta$ parameter for the spinal cord was taken from Schultheiss [45].

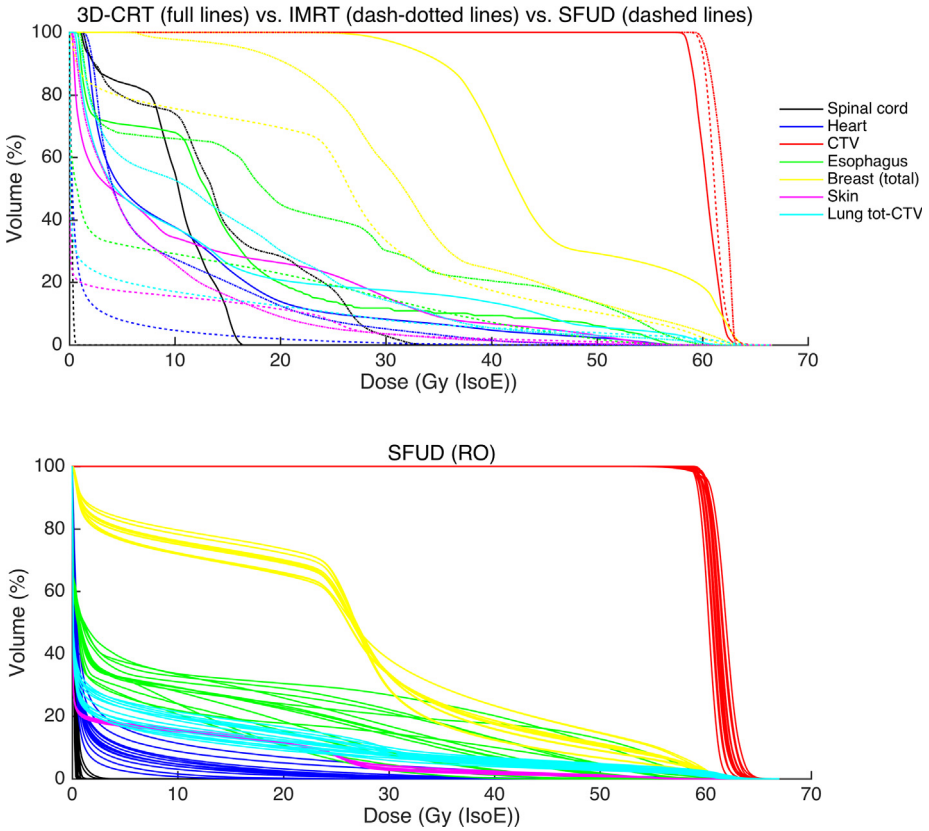


**Fig. 2.** DVHs calculated for the 3D-CRT, IMRT and SFUD plans. Upper panel: comparison of 3D-CRT plans (full lines) vs. IMRT plans (dash-dotted lines) vs. nominal SFUD plans (dashed lines); lower panel: uncertainty DVHs for all the simulated scenarios of the SFUD plan. Data is for patient #1.

with the nominal SFUD plans and both the 3D-CRT and the IMRT plans ($p > 0.05$), Table 4. For the worst-case scenario of the SFUD plans, lower or comparable dose-volume values were obtained for all OARs, when compared to the 3D-CRT or the IMRT plans, except for the maximum doses given to the oesophagus and to the skin. The maximum dose given to the oesophagus decreased from a median value of 57.6 Gy (RBE) with the worst-case scenario SFUD plans, to median values of 53.5 Gy with 3D-CRT ($p < 0.05$) and 53.6 Gy with IMRT ($p < 0.05$). For the skin, a median value of the maximum dose of 51.1 Gy (RBE) was obtained with the worst-case scenario of the SFUD plans. This value was reduced to a median value of 46.6 Gy with the 3D-CRT plans ($p < 0.05$), while with the IMRT plans no significant difference was observed ($p > 0.05$).

A summary of the obtained dosimetric volumes with the 3D-CRT, IMRT, and the SFUD (nominal and worst-case scenario) plans is presented in Table 4.

### 3.2. NTCP comparison

A summary of the calculated NTCP values, obtained with the 3D-CRT, IMRT and SFUD plans for the different toxicities evaluated, is shown in Table 5. The nominal SFUD plans were associated with significantly lower risk of pneumonitis (median 2.5%), compared to 3D-CRT (median 9.1%) and IMRT (median 10.8%), $p < 0.05$. The risk of myelopathy was reduced from a median value of 0.4% with 3D-CRT to 0% with the nominal SFUD plans ($p < 0.05$). For the worst-case scenario SFUD plans, significantly lower risk of pneumonitis (median 3.3%) was registered, compared to 3D-CRT (median 9.1%) and IMRT (median 10.8%), $p < 0.05$. The risk of myelopathy was also lower with the worst-case scenario SFUD plans, compared to the 3D-CRT (0% vs. 0.4%), $p < 0.05$. Lower risk of esophagitis was calculated for the worst-case scenario SFUD plans (median 4.3%), compared to the IMRT plans (median 5.8%), $p < 0.05$. The risks of pericarditis and RT-induced skin toxicity (RIST) were non-existent with all three modalities (3D-CRT, IMRT, nominal and worst-case scenario of the SFUD plans), $p > 0.05$.

## 4. Discussion

In the present study, we demonstrate dosimetric advantages of using SFUD delivered with scanned proton beams in the treatment of thymic tumours, as compared to photon 3D-CRT and IMRT. The probability of observing different toxicities was also evaluated for the three treatment modalities. A good CTV dose-coverage was obtained with both the SFUD plans and the clinically used photon plans. The dose-volume values for several OARs were significantly lower with the SFUD plans, than in the corresponding 3D-CRT and IMRT plans. This resulted in lower estimated NTCPs with SFUD for the lung, spinal cord, and oesophagus.

In general, the dose reductions with the SFUD plans were observed for the mean doses given to most of the OARs, while there were no differences in maximum doses, except for the spinal cord. This fact was observed as the integral doses with PBT can be expected to be lower. However, the maximum doses, in particular for the OARs located in close proximity of the target volumes, will be of comparable values as for the photon plans. Similar findings were observed in comparative studies of photon- and proton-RT for liver targets [14,15] where the potential dose-reduction with proton-beams was evident in the low and intermediate dose ranges.

In our study, doses to the lungs and oesophagus were significantly reduced in favour of SFUD, which correlated to clinically significant relative reductions in NTCP for pneumonitis and esophagitis. Minimizing exposure to lung and oesophagus seems important since complications in these OARs appear to be quite common. A recent study

**Table 4**
Dosimetric comparison between the 3D-CRT, IMRT and the SFUD plans for the CTV and OARs. Proton doses are presented in Gy (RBE). IQR = inter quartile range.

| Target/OAR | Parameter | 3D-CRT (median and IQR) | IMRT (median and IQR) | SFUD (median and IQR) | | Relative reduction with the SFUD plans in relation to the 3D-CRT and IMRT plans (%) | | | |
|---|---|---|---|---|---|---|---|---|---|
| | | | | Nominal plans | Worst-case scenario OARs** | Nominal plans | | Worst-case scenario OARs** | |
| | | | | | | 3D-CRT | IMRT | 3D-CRT | IMRT |
| CTV | D98 (%) | 97 (96.3–98.0) | 98.7 (97.1–99.4) | 99 (98–99.8) | – | −2.0* | −0.3* | – | – |
| | D2 (%) | 110 (110–111) | 104.8 (104.6–105.0) | 106 (105–107.8) | – | 3.6* | −1.1* | – | – |
| Spinal Cord | Dmax (Gy) | 40.2 (17.3–42.4) | 27.0 (25.2–33.3) | 3.2 (0.3–12.0) | 11.3 (0.5–26.2) | 92.0 | 88.3 | 71.9 | 58.1 |
| Oesophagus | Dmean (Gy) | 20.2 (11.8–24.3) | 17.9 (14.4–22.6) | 7.6 (1.5–18.9) | 9.2 (4.6–15.2) | 62.4 | 57.7 | 54.5 | 48.5 |
| | Dmax (Gy) | 53.5 (41.3–57.0) | 53.6 (47.7–58.4) | 53.8 (31.3–59.6) | 57.6 (53.4–60.5) | −0.6* | −0.3* | −7.6 | −77.4 |
| | V30 (%) | 41.5 (13.5–47.5) | 24.2 (16.1–38.2) | 11.8 (0–32.2) | 14.3 (3.6–26.8) | 71.6 | 51.2 | 65.7 | 41.1 |
| Heart | Dmean (Gy) | 9.3 (1.7–11.6) | 8.8 (2.0–10.6) | 1.5 (0.2–6.7) | 3.3 (0.9–7.8) | 83.9 | 83.0 | 65.1 | 63.1 |
| | V5 (%) | 25.0 (2.3–40.3) | 28.0 (3.6–36.1) | 7.5 (1.0–17.2) | 13.3 (4.2–19.9) | 70.0 | 73.3 | 47.0* | 52.6* |
| | V30 (%) | 9.0 (0–16.8) | 6.2 (0.0–13.5) | 1.3 (0–10.6) | 3.5 (0–13.8) | 85.6 | 79.0 | 61.7* | 44.4* |
| | V45 (%) | 3.5 (0–9.5) | 2.0 (0.0–9.1) | 0.4 (0–6.6) | 1.3 (0–7.9) | 88.6 | 80.0 | 64.3* | 37.5* |
| LAD | Dmean (Gy) | 22.5 (10.3–31.0) | 25.4 (12.4–30.5) | 12.0 (1.1–31.1) | 17.3 (3.9–30.4) | 46.7 | 52.9 | 23.3* | 32.0* |
| | Dmax (Gy) | 48.5 (32.0–58.9) | 40.9 (21.5–59.8) | 33.1 (4.2–58.9) | 50.2 (13.5–60.2) | 31.8* | 19.1* | −3.4* | −22.8* |
| Lung (total)-CTV | Dmean (Gy) | 13.4 (10.8–16.1) | 14.7 (13.2–16.7) | 5.8 (4.7–8.7) | 6.5 (5.7–9.0) | 56.7 | 60.8 | 51.5 | 55.6 |
| | V5 (%) | 55.5 (47.3–62.8) | 60.1 (54.5–71.2) | 20.0 (16.0–33.8) | 22.6 (19.9–35.2) | 64.0 | 66.7 | 59.4 | 62.5 |
| | V20 (%) | 22.0 (17.0–29.3) | 31.3 (23.8–35.2) | 10.5 (8.3–15.8) | 12.3 (9.6–15.4) | 52.3 | 66.4 | 44.1 | 60.6 |
| Skin | Dmax (Gy) | 46.9 (40.5–54.6) | 44.4 (35.5–53.4) | 50.6 (48.2–52.6) | 51.1 (48.9–53.0) | −7.9* | −14.1* | −9.0 | −15.2* |
| Breast (total) | Dmean (Gy) | 15.6 (10.2–30.4) | 15.4 (13.7–20.5) | 8.6 (5.5–12.8) | 8.2 (5.1–10.6) | 44.9 | 44.3 | 47.4 | 46.6 |
| | Dmax (Gy) | 51.7 (49.3–58.6) | 54.7 (45.8–56.2) | 51.2 (47.5–55.4) | 52.6 (50.7–55.9) | 1.0* | 6.4* | −1.7* | 3.8* |

** The worst-case scenario for the OARs refers to the scenario representing the highest dose-volume curve

* $p > 0.05$; otherwise $p < 0.05$. The pairwise comparison was done between the dose-volume values taken from the SFUD plans and the photon plans (3D-CT and IMRT plans).

**Table 5**
Median NTCP values obtained with 3D-CRT, IMRT and SFUD plans.

| OAR | Endpoint | NTCP (%) [median value and IQR] | | | |
|---|---|---|---|---|---|
| | | 3D-CRT | IMRT | SFUD | |
| | | | | Nominal plans | Worst-case scenario |
| Heart | Pericarditis | 0 | 0 | 0[‡,†] | 0[‡,†] |
| Lung | Pneumonitis | 9.1 (6.0–13.1) | 10.8 (8.7–14.2) | 2.5 (2.0–4.3) | 3.3 (2.8–5.3) |
| Spinal Cord | Myelopathy | 0.4 (0–1.2) | 0 | 0 | 0 |
| Oesophagus | Esophagitis | 7.1 (1.7–14.5) | 5.8 (3.5–12.4) | 1.5 (0.1–2.9) [‡,†] | 4.3 (1.0–10.3)[‡] |
| Skin | RIST | 0 | 0 | 0[‡,†] | 0[‡,†] |

[‡,†] $p > 0.05$; otherwise $p < 0.05$. The pairwise comparison was done between the SFUD plans and the photon plans ([‡]3D-CT and [†]IMRT plans).

has reported up to 25% Grade 3–4 esophagitis and 12.5% Grade 3–4 pneumonitis, in patients treated with definitive concurrent chemoradiotherapy for locally advanced thymic tumours [16].

For OARs with a parallel organisation, such as the lungs and breasts, it is probably most important to avoid high mean doses, while in OARs which are serially organized, *e.g.,* oesophagus and spinal cord, avoidance of high maximum doses is more important [17]. The heart, because of its complex organisation, with both parallel and serially organized sub units, is more difficult to assess in this regard. For this reason, it is probably preferable to present additional DVH-parameters for this particular OAR. It is a well-known fact that incidental irradiation of the heart increases the subsequent risk of coronary heart disease and cardiac death [18,19]. It is not known, however, if this is mainly due to damage to the myocardial microvasculature or the larger coronary arteries, *e.g.*, LAD. Darby et al. conducted a population-based study on cardiovascular events in more than 2000 women, who had been treated with RT for breast cancer [20]. In this study, the mean dose given to the heart was better correlated to cardiovascular events than the mean dose to LAD, suggesting that it is after all more important to lower total exposure to the entire heart, than to particular subunits, *e.g.,* coronary arteries. In our study, the mean dose to the heart was reduced by more than 80%. Although some suggestions have been made regarding constraints for LAD, [21], most publications on RT, which includes heart exposure, do not report such values. In our study we did not include any constraints for the LAD.

Dose-surface maps (DSM), generated from dose distribution data, may improve our understanding of which parts of different OARs that are more sensitive for toxicity, and whether high maximum or high mean doses are most important for a particular area. So far DSM-analysis are mostly used in pelvic irradiation [22–24] but should in future studies also be used in thoracic radiotherapy, and for comparison of different treatment modalities.

A small number of treatment studies have demonstrated PBT as a feasible alternative to photon RT in the treatment of thymic tumours. Parikh et al. compared dosimetric differences between passive scattering PBT and alternative IMRT-plans in 4 pts treated with adjuvant PBT for thymomas [7]. Target coverage was adequate, and the mean doses given to heart, lung, oesophagus, and breast were significantly lower in the PBT-plans. Short-term follow-up (FU) showed minimal acute toxicities (Grade 1–2 dermatitis). Vogel et al. used double scattering (DS-) PBT as adjuvant, salvage or definitive treatment in 27 pts with thymic tumours [8]. PTV-coverage was excellent and doses to OARs, such as lung, heart, LAD, oesophagus, and skin appeared to be low, although no comparison to alternative photon plans were presented. A medium 2-year FU showed low rates of toxicity and 100% local control. Furthermore, a few case reports have also been published demonstrating lower doses to OARs using PBT as an alternative to photon RT [25,26].

Several studies comparing PBT to 3D-CRT and IMRT for different thoracic tumours have demonstrated dosimetric advantages in favor of PBT. Hoppe et al [27] compared planned doses to several cardiac subunits, for the 3 modalities, for 13 pts with mediastinal Hodgkins lymphoma. Mean doses to all major cardiac subunits were reduced with PBT, as compared to 3D-CRT and IMRT. Ling et al [28] compared doses to several OARs for 10 pts with oesophageal cancer, for the 3 modalities. The results demonstrate a significant benefit of PBT, in regard to lower doses to several OARs, especially heart and lungs. Also for lung cancer treatment, a few studies have shown dosimetric advantages with PBT, as compared to both 3D-CRT and IMRT [29,30]. The results of these studies are in accordance with our results.

In the studies comparing photon- and proton-RT for thymic cancer [7,8], the proton plans were performed using the DS approach, in which the proton range and setup uncertainties were considered through the use of adequate compensators and apertures. As the scanned-proton SFUD was implemented in our study, these proton-specific uncertainties were taken into account in a more sophisticated manner. The importance of implementing strategies to achieve plan robustness in PBT has been highlighted [31–33]. In our study, the planning for PBT was performed using the fsPTV, which has been shown to achieve robust plans in the presence of proton-specific uncertainties [34]. Furthermore, a robust optimization was also performed to account for setup and range uncertainties, which resulted in more realistic and robust proton plans. This was observed when comparing the obtained dose-volume values and the NTCPs obtained with the photon plans, with the values calculated for the worst-case scenario of the SFUD plans for the OARs. The worst-case scenario of the SFUD plans resulted in similar or improved plans for most of the OARs, compared to both the 3D-CRT and IMRT plans (Tables 4 and 5).

The delivery of PBT to thoracic tumours with scanned beams demands that approaches to mitigate organ motion are also implemented. Organ motion, when using scanned proton beams, is the source of the interplay effect, loss of sharpness of the dose gradients and dose deformation due to density changes along the beam path. The impact of organ motion on the quality of the dose distributions produced by scanned proton beams has been extensively discussed in the study by, *e.g.*, Bert and Durante [35], and can result in under-dosage of the target volume and over-dosage of the OARs surrounding the target volume. This would ultimately lead to the reduction of the dosimetric advantages (and the advantages in terms of NTCP reduction) of the proton beams. The plans used in our study were prepared on static CT image sets, disregarding the effects of organ motion for the SFUD plans. However, the use of robust optimisation has been shown to considerably improve the plan quality in the presence of organ motion [36,37]. Motion mitigation strategies such as the use of image-guidance, motion control through gating, and possibly in the future tracking, will further improve the safety in the delivery of treatments with scanned proton beams.

In RT of thoracic and mediastinal tumours, not only acute and late toxicities are of interest, but also the risk of RT-induced secondary malignant neoplasms (SMN), since long-term survival in many patients with thymomas is to be expected. Some of the OARs of interest are also prone to cancer development, *e.g.,* lung, oesophagus, breast, and skin.

Vogel et al. assessed the risk of SMNs following adjuvant DS-PBT as compared to IMRT in 10 pts with stage II thymoma [38]. The calculated risk of SMNs in lung, esophagus, breast, skin, and stomach was significantly lower in DS-PBT as compared to IMRT. The comparison of the expected risk for SMN between 3D-CRT, IMRT, and SFUD, for the patients included in the present report, is part of our future study. The use of spot-scanning PBT, which, due to lower production of secondary neutrons and better target dose-conformity compared to DS-PBT, may have the potential to further reduce the risk of SMNs [39].

## 5. Conclusion

The present study confirms the dosimetric advantage of using PBT in the treatment of thymic tumours, as compared to 3D-CRT and IMRT, in regard to lower doses to OARs, and in reducing the risk of toxicity, especially to the lung and oesophagus. Randomized, prospective studies, comparing PBT with photon radiotherapy, should be performed to confirm PBT as a feasible alternative in the treatment of thymic tumours.

## Acknowledgements

**Declarations of interest**: None.

**Funding**: this research did not receive any specific grant from funding agencies in the public, commercial, or not-for profit sectors. Gracinda Mondlane and Albert Siegbahn would like to acknowledge the support of the cancer research funds of Radiumhemmet.

## References

[1] Suster S, Moran CA. Histologic classification of thymoma: the World Health Organization and beyond. Hematol Oncol Clin North Am 2008;22:381–92.
[2] Ettinger DS, Riely GJ, Akerley W, Borghaei H, Chang AC, Cheney RT, et al. Thymomas and thymic carcinomas: clinical practice guidelines in oncology. J Natl Compr Canc Netw 2013;11:562–76.
[3] Gagliardi G, Constine LS, Moiseenko V, Correa C, Pierce LJ, Allen AM, et al. Radiation dose-volume effects in the heart. Int J Radiat Oncol Biol Phys 2010;76:S77–85.
[4] Kirkpatrick JP, van der Kogel AJ, Schultheiss TE. Radiation dose-volume effects in the spinal cord. Int J Radiat Oncol Biol Phys 2010;76:S42–9.
[5] Marks LB, Bentzen SM, Deasy JO, Kong FM, Bradley JD, Vogelius IS, et al. Radiation dose-volume effects in the lung. Int J Radiat Oncol Biol Phys 2010;76:S70–6.
[6] Werner-Wasik M, Yorke E, Deasy J, Nam J, Marks LB. Radiation dose-volume effects in the esophagus. Int J Radiat Oncol Biol Phys 2010;76:S86–93.
[7] Parikh RR, Rhome R, Hug E, Tsai H, Cahlon O, Chon B, et al. Adjuvant proton beam therapy in the management of thymoma: a dosimetric comparison and acute toxicities. Clinical lung cancer 2016;17:362–6.
[8] Vogel J, Berman AT, Lin L, Pechet TT, Levin WP, Gabriel P, et al. Prospective study of proton beam radiation therapy for adjuvant and definitive treatment of thymoma and thymic carcinoma: early response and toxicity assessment. Radiotherapy Oncol. 2016;118:504–9.
[9] Jia Y, Zhao L, Cheng CW, McDonald MW, Das IJ. Dose perturbation effect of metallic spinal implants in proton beam therapy. J Appl Clin Med Phys 2015;16:333–43.
[10] Paganetti H, van Luijk P. Biological considerations when comparing proton therapy with photon therapy. Seminars Radiation Oncol. 2013;23:77–87.
[11] ICRU. ICRU Report 83: Prescribing, recording, and reporting photon-beam intensity modulated radiotherapy (IMRT). Journal of the International Commission on Radiation Units and Measurements. 2010;10.
[12] Kutcher GJ, Burman C. Calculation of complication probability factors for non-uniform normal tissue irradiation: the effective volume method. Int J Radiat Oncol Biol Phys 1989;16:1623–30.
[13] Lyman JT. Complication probability as assessed from dose-volume histograms. Radiat Res Suppl 1985;8:S13–9.
[14] Petersen JB, Lassen Y, Hansen AT, Muren LP, Grau C, Hoyer M. Normal liver tissue sparing by intensity-modulated proton stereotactic body radiotherapy for solitary liver tumours. Acta Oncol 2011;50:823–8.
[15] Mondlane G, Gubanski M, Lind PA, Henry T, Ureba A, Siegbahn A. Dosimetric comparison of plans for photon- or proton-beam based radiosurgery of liver metastases. Int J Particle Therapy 2016;3:277–84.
[16] Wang CL, Gao LT, Lv CX, Zhu L, Fang WT. Outcome of nonsurgical treatment for locally advanced thymic tumors. J Thorac Dis 2016;8:705–10.
[17] Marks LB, Yorke ED, Jackson A, Ten Haken RK, Constine LS, Eisbruch A, et al. Use of normal tissue complication probability models in the clinic. Int J Radiat Oncol Biol Phys 2010;76:S10–9.
[18] Cheng YJ, Nie XY, Ji CC, Lin XX, Liu LJ, Chen XM, et al. Cardiovascular risk after radiotherapy in women With. Breast Cancer J Am Heart Assoc 2017;6..
[19] McGale P, Darby SC, Hall P, Adolfsson J, Bengtsson NO, Bennet AM, et al. Incidence of heart disease in 35,000 women treated with radiotherapy for breast cancer in Denmark and Sweden. Radiotherapy Oncol 2011;100:167–75.
[20] Darby SC, Ewertz M, McGale P, Bennet AM, Blom-Goldman U, Bronnum D, et al. Risk of ischemic heart disease in women after radiotherapy for breast cancer. N Engl J Med 2013;368:987–98.
[21] Nielsen MH, Berg M, Pedersen AN, Andersen K, Glavicic V, Jakobsen EH, et al. Delineation of target volumes and organs at risk in adjuvant radiotherapy of early breast cancer: national guidelines and contouring atlas by the Danish Breast Cancer Cooperative Group. Acta Oncol 2013;52:703–10.
[22] Improta I, Palorini F, Cozzarini C, Rancati T, Avuzzi B, Franco P, et al. Bladder spatial-dose descriptors correlate with acute urinary toxicity after radiation therapy for prostate cancer. Phys Med 2016;32:1681–9.
[23] Landoni V, Fiorino C, Cozzarini C, Sanguineti G, Valdagni R, Rancati T. Predicting toxicity in radiotherapy for prostate cancer. Phys Med 2016;32:521–32.
[24] Palorini F, Botti A, Carillo V, Gianolini S, Improta I, Iotti C, et al. Bladder dose-surface maps and urinary toxicity: Robustness with respect to motion in assessing local dose effects. Phys Med 2016;32:506–11.
[25] Figura N, Hoppe BS, Flampouri S, Su Z, Osian O, Monroe A, et al. Postoperative proton therapy in the management of stage III thymoma. J Thoracic Oncol 2013;8:e38–40.
[26] Kojima H, Isaka M, Nagata M, Onoe T, Murayama S, Ohde Y. Preoperative proton beam therapy for thymoma: a case report. Ann Thorac Cardiovasc Surg 2016;22:186–8.
[27] Hoppe BS, Flampouri S, Su Z, Latif N, Dang NH, Lynch J, et al. Effective dose reduction to cardiac structures using protons compared with 3DCRT and IMRT in mediastinal Hodgkin lymphoma. Int J Radiat Oncol Biol Phys 2012;84:449–55.
[28] Ling TC, Slater JM, Nookala P, Mifflin R, Grove R, Ly AM, et al. Analysis of Intensity-Modulated Radiation Therapy (IMRT), proton and 3D Conformal Radiotherapy (3D-CRT) for reducing perioperative cardiopulmonary complications in esophageal cancer patients. Cancers (Basel) 2014;6:2356–68.
[29] Roelofs E, Engelsman M, Rasch C, Persoon L, Qamhiyeh S, de Ruysscher D, et al. Results of a multicentric in silico clinical trial (ROCOCO): comparing radiotherapy with photons and protons for non-small cell lung cancer. J Thoracic Oncol 2012;7:165–76.
[30] Chang JY, Zhang X, Wang X, Kang Y, Riley B, Bilton S, et al. Significant reduction of normal tissue dose by proton radiotherapy compared with three-dimensional conformal or intensity-modulated radiation therapy in Stage I or Stage III non-small-cell lung cancer. Int J Radiat Oncol Biol Phys 2006;65:1087–96.
[31] Fredriksson A, Forsgren A, Hardemark B. Minimax optimization for handling range and setup uncertainties in proton therapy. Med Phys 2011;38:1672–84.
[32] Arts T, Breedveld S, de Jong MA, Astreinidou E, Tans L, Keskin-Cambay F, et al. The impact of treatment accuracy on proton therapy patient selection for oropharyngeal cancer patients. Radiotherapy Oncol 2017;125:520–5.
[33] Yoshimura T, Kinoshita R, Onodera S, Toramatsu C, Suzuki R, Ito YM, et al. NTCP modeling analysis of acute hematologic toxicity in whole pelvic radiation therapy for gynecologic malignancies – A dosimetric comparison of IMRT and spot-scanning proton therapy (SSPT). Phys Med 2016;32:1095–102.
[34] Park PC, Zhu XR, Lee AK, Sahoo N, Melancon AD, Zhang L, et al. A beam-specific planning target volume (PTV) design for proton therapy to account for setup and range uncertainties. Int J Radiat Oncol Biol Phys 2012;82:e329–36.
[35] Bert C, Durante M. Motion in radiotherapy: particle therapy. Phys Med Biol 2011;56:R113–44.
[36] Li H, Zhang X, Park P, Liu W, Chang J, Liao Z, et al. Robust optimization in intensity-modulated proton therapy to account for anatomy changes in lung cancer patients. Radiotherapy Oncol 2015;114:367–72.
[37] Liu W, Liao Z, Schild SE, Liu Z, Li H, Li Y, et al. Impact of respiratory motion on worst-case scenario optimized intensity modulated proton therapy for lung cancers. Pract Radiat Oncol 2015;5:e77–86.
[38] Vogel J, Lin L, Litzky LA, Berman AT, Simone 2nd CB. Predicted rate of secondary malignancies following adjuvant proton versus photon radiation therapy for thymoma. Int J Radiat Oncol Biol Phys 2017;99:427–33.
[39] Hall EJ. Intensity-modulated radiation therapy, protons, and the risk of second cancers. Int J Radiat Oncol Biol Phys 2006;65:1–7.
[40] Martel MK, Sahijdak WM, Ten Haken RK, Kessler ML, Turrisi AT. Fraction size and dose parameters related to the incidence of pericardial effusions. Int J Radiat Oncol Biol Phys 1998;40:155–61.
[41] Chapet O, Kong FM, Lee JS, Hayman JA, Ten Haken RK. Normal tissue complication probability modeling for acute esophagitis in patients treated with conformal radiation therapy for non-small cell lung cancer. Radiotherapy Oncol 2005;77:176–81.
[42] Pastore F, Conson M, D'Avino V, Palma G, Liuzzi R, Solla R, et al. Dose-surface analysis for prediction of severe acute radio-induced skin toxicity in breast cancer patients. Acta Oncol 2016;55:466–73.
[43] Semenenko VA, Li XA. Lyman-Kutcher-Burman NTCP model parameters for radiation pneumonitis and xerostomia based on combined analysis of published clinical data. Phys Med Biol 2008;53:737–55.
[44] Burman C, Kutcher GJ, Emami B, Goitein M. Fitting of normal tissue tolerance data to an analytic function. Int J Radiat Oncol Biol Phys 1991;21:123–35.
[45] Schultheiss TE. The radiation dose-response of the human spinal cord. Int J Radiat Oncol Biol Phys 2008;71:1455–9.